Thermal soaring over the North Sea and implications for wind farm interactions

Section S1. Species distribution in study area

The ESAS 5.0 (European Seabirds at Sea) database is a ship survey database (Reid & Camphuysen 1998) that incorporates all observational data made through a standardized protocol (Camphuysen et al. 2004) and is maintained by the NWO-NIOZ Royal Netherlands Institute for Sea Research. The database was queried on 4 January 2022 for all bird species observed in flight in the months of June and July in the area near Luchterduinen radar (Table S1) and Gemini radar (Table S2). For Luchterduinen, data was sampled between 52.15-52.65°N, 3.5-4.5°E, which describes a rectangular area around the radar (52.427827°N, 4.185345°E). For Gemini, data was sampled between 53.75-54.25°N, 5-7°E, which describes a rectangular area around the radar (54.036983°N, 6.041655°E). For readability, all species with an observation rate below 0.1% have been omitted from the table.
Gemini has 657 km^2 surveyed (2.237 km steamed on effort), with data collected between 1987 and 2012. Luchterduinen has 1607 km^2 surveyed (5354 km steamed on effort), with data originating from the same period.

Table S1 Number of birds observed in flight and percentage of total per species in the months of June and July from 1987 - 2012 in the area near wind farm Luchterduinen between 52.15-52.65°N, 3.5-4.5°E. Data was queried on 4 January 2022. For readability, all species with an observation rate below 0.1% have been omitted

Species ID	Species name	Scientific name	Birds (#)	Percentage of total (%)
5910	Lesser Black-backed Gull	*Larus fuscus*	10818	65
720	Great Cormorant	*Phalacrocorax carbo*	1551	9.4
5920	Herring Gull	*Larus argentatus*	1297	7.9
5919	Herring Gull / Lesser Black-backed Gull	*L. argentatus / L. fuscus*	901	5.5
6005	large gull	*Larus spec.*	369	2.2
2130	Black Scoter	*Melanitta nigra*	270	1.6
220	Northern Fulmar	*Fulmarus glacialis*	228	1.4
710	Northern Gannet	*Sula bassana*	170	1.0
6020	Black-legged Kittiwake	*Rissa tridactyla*	170	1.0
6000	Great Black-backed Gull	*Larus marinus*	133	0.8
5820	Black-headed Gull	*Larus ridibundus*	116	0.7
6110	Sandwich Tern	*Sterna sandvicensis*	112	0.7
5900	Common Gull	*Larus canus*	88	0.5
7950	Common Swift	*Apus apus*	55	0.3
15820	Common Starling	*Sturnus vulgaris*	49	0.3
6150	Common Tern	*Sterna hirundo*	35	0.2
6160	Arctic Tern	*Sterna paradisaea*	26	0.2
1730	Common Shelduck	*Tadorna tadorna*	18	0.1
5410	Eurasian Curlew	*Numenius arquata*	17	0.1
4500	Eurasian Oystercatcher	*Haematopus ostralegus*	14	0.1

Table S2 Number of birds observed in flight and percentage of total per species in the months of June and July from 1987 – 2012 in the area near Gemini wind park between 53.75-54.25°N, 5-7°E. Data was queried on 04 January 2022. For readability, all species with an observation rate below 0.1% have been omitted

Species ID	Species name	Scientific name	Birds (#)	Percentage of total (%)
5910	Lesser Black-backed Gull	*Larus fuscus*	1426	76.7
6020	Black-legged Kittiwake	*Rissa tridactyla*	157	8.4
710	Northern Gannet	*Sula bassana*	77	4.1
220	Northern Fulmar	*Fulmarus glacialis*	47	2.5
2130	Black Scoter	*Melanitta nigra*	37	2.0
6160	Arctic Tern	*Sterna paradisaea*	19	1.0
7950	Common Swift	*Apus apus*	19	1.0
6340	Common Guillemot	*Uria aalge*	15	0.8
5820	Black-headed Gull	*Larus ridibundus*	12	0.6
6110	Sandwich Tern	*Sterna sandvicensis*	9	0.5
5690	Great Skua	*Stercorarius skua*	7	0.4
5900	Common Gull	*Larus canus*	5	0.3
5920	Herring Gull	*Larus argentatus*	5	0.3
6000	Great Black-backed Gull	*Larus marinus*	5	0.3
15820	Common Starling	*Sturnus vulgaris*	3	0.2
5610	Ruddy Turnstone	*Arenaria interpres*	2	0.1
5670	Arctic Skua	*Stercorarius parasiticus*	2	0.1
460	Manx Shearwater	*Puffinus puffinus*	1	0.1
720	Great Cormorant	*Phalacrocorax carbo*	1	0.1
1220	Grey Heron	*Ardea cinerea*	1	0.1

Section S2. Overview of UvA-BiTs logger data per individual per year

Table S3 Summary table of data collected for each tagged lesser black-backed gull per year. The same individual number over a different year indicates a returned individual. Total time indicates the sum of all time intervals for the recorded GPS measurements.

Colony	Individual	Year	No. GPS measurements	Total time (Hr)
IJmuiden	5963	2019	16024	22.33
IJmuiden	5962	2019	24696	34.36
IJmuiden	5861	2019	28130	39.27
IJmuiden	5584	2019	16264	22.62
IJmuiden	5579	2019	45615	63.47
IJmuiden	5565	2019	15698	21.86
IJmuiden	5491	2019	25792	35.86
IJmuiden	5441	2019	39738	55.28
IJmuiden	5433	2019	20796	28.98
IJmuiden	5369	2019	24938	34.68
Schiermonnikoog	5709	2019	1063	1.8
Schiermonnikoog	5561	2019	1731	2.26
Schiermonnikoog	5560	2019	3059	4.06
Schiermonnikoog	5555	2019	3155	3.9
Schiermonnikoog	5554	2019	5866	7.4
Schiermonnikoog	5532	2019	26745	33.98
Schiermonnikoog	5525	2019	25368	30.97
Schiermonnikoog	5524	2019	16583	20.62
IJmuiden	5983	2020	19152	26.65
IJmuiden	5979	2020	4693	6.53
IJmuiden	5977	2020	10561	14.72
IJmuiden	5971	2020	4655	6.47
IJmuiden	5967	2020	2048	2.85
IJmuiden	5964	2020	2010	2.8
IJmuiden	5861	2020	1216	1.69
IJmuiden	5579	2020	34928	48.6
IJmuiden	5576	2020	10671	14.89
IJmuiden	5557	2020	20043	27.88
Schiermonnikoog	5780	2020	11143	18.91
Schiermonnikoog	5709	2020	2016	3.41
Schiermonnikoog	5560	2020	16624	19
Schiermonnikoog	5554	2020	41071	47.02
Schiermonnikoog	5533	2020	11765	13.57
Schiermonnikoog	5532	2020	72671	83.45
Schiermonnikoog	5527	2020	7814	9.16
Schiermonnikoog	5526	2020	228	0.26
Schiermonnikoog	5524	2020	10052	11.62

Section S3. RobinRadar 3D Fixed detection probability at different range and heights.

Figure S1 shows the range and altitude from the radar at which the probability of detection for an object of 1 standard avian target (SAT, Figure S1a) and 0.125 SAT (Figure S1b) by the horizontal S-band antenna of the RobinRadar 3D Fixed system is > 80%. A SAT is a theoretical object used as a standard for evaluating the performance of avian radar systems and approximates the physical features of a carrion crow (*Corvus corone*) with a radar cross section (RCS) of -16 dB m^2 and a mass of 500 g. A 0.125 SAT object correlates to a RCS of -25 dB m^2 and a mass of 62.5 g, the size of a song thrush (*Turdus philomelos*).

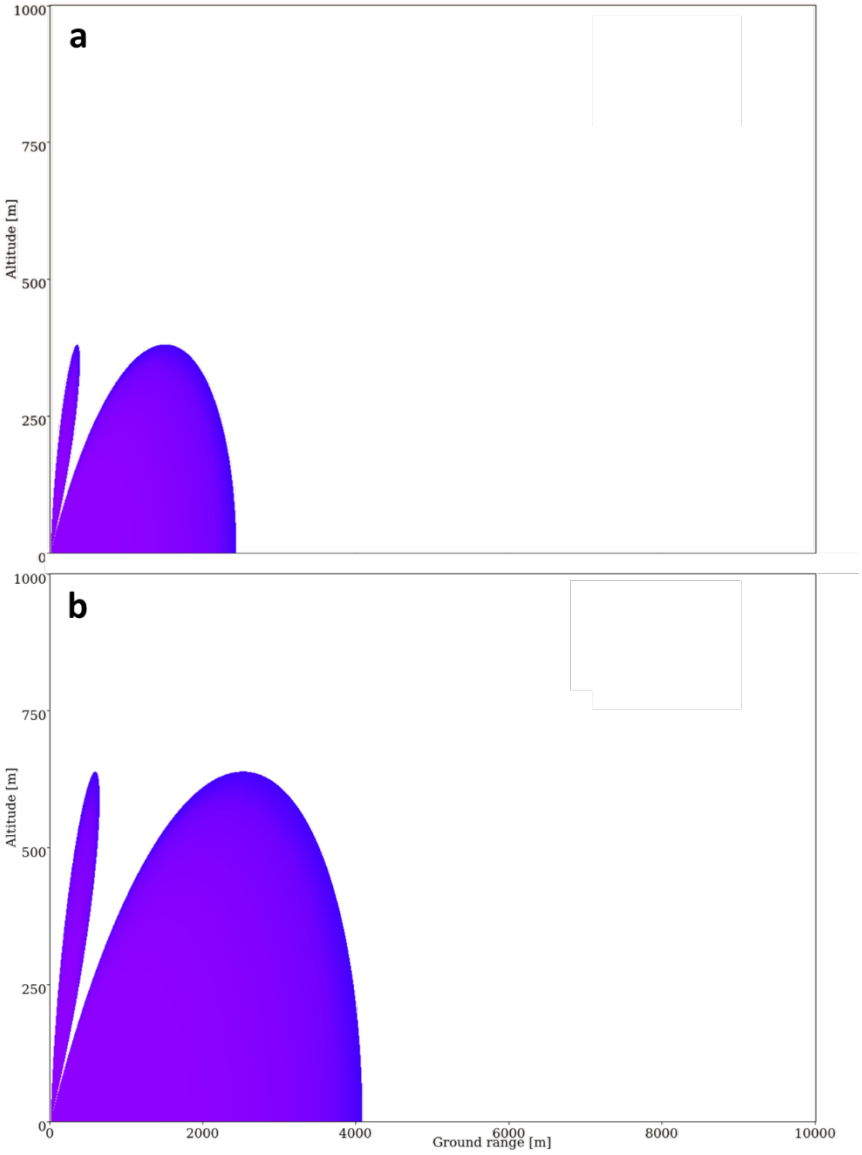

Figure S1 Probability of detection by the horizontal S-band antenna of the RobinRadar 3D-fix at different ground range and altitude from the radar position (0,0 on the axes). (a) The area shows the range/altitude combinations at which the probability of detection > 80%. Probability of detecting a target of size 1 SAT. (b) Probability of detecting a target of size 0.125 SAT. Colour scale shows theoretical detection probability ranging from 100% (purple) to 80% (blue). Figures provided by RobinRadar

Section S4. Accounting for detection bias caused by dynamic radar filtering

The dynamic filter activity in each radar image directly affected detection probability of birds by increasing the threshold at which objects are detected. The filter is always active, ranging from 0 (no filtering) to 1 (complete filtering). The number of bird observations per hour is negatively related to the filter activity (black dots, Figure S2) and could affect the outcome of modelling efforts through inclusion of unreliable observation hours. Firstly, the estimated effect of the hourly averaged dynamic filtering on bird observations was modelled through Generalized Additive Modelling (GAM). Hourly bird count was used as the dependent variable, with hourly average filter activity as predictor (thin plate regression spline smoother, k = 5 to prevent overfitting), and assuming a Gaussian distribution of the model error. The estimated effect showed a decrease in bird count around filter activity = 0.1 (blue line, Figure S2), which levelled out around filter activity = 0.35. The filter activity at which this levelling out process starts was taken as the threshold above which hourly bird counts were considered highly affected. This value was found by calculating the second derivative over the estimated effect (red line, Figure S2) and finding the filter activity at the maximum of the curve (red dashed line, Figure S2). This threshold was 0.327 for Luchterduinen radar and 0.311 for Gemini radar; observation hours in which the average filter activity was higher than the threshold were excluded from further analysis.

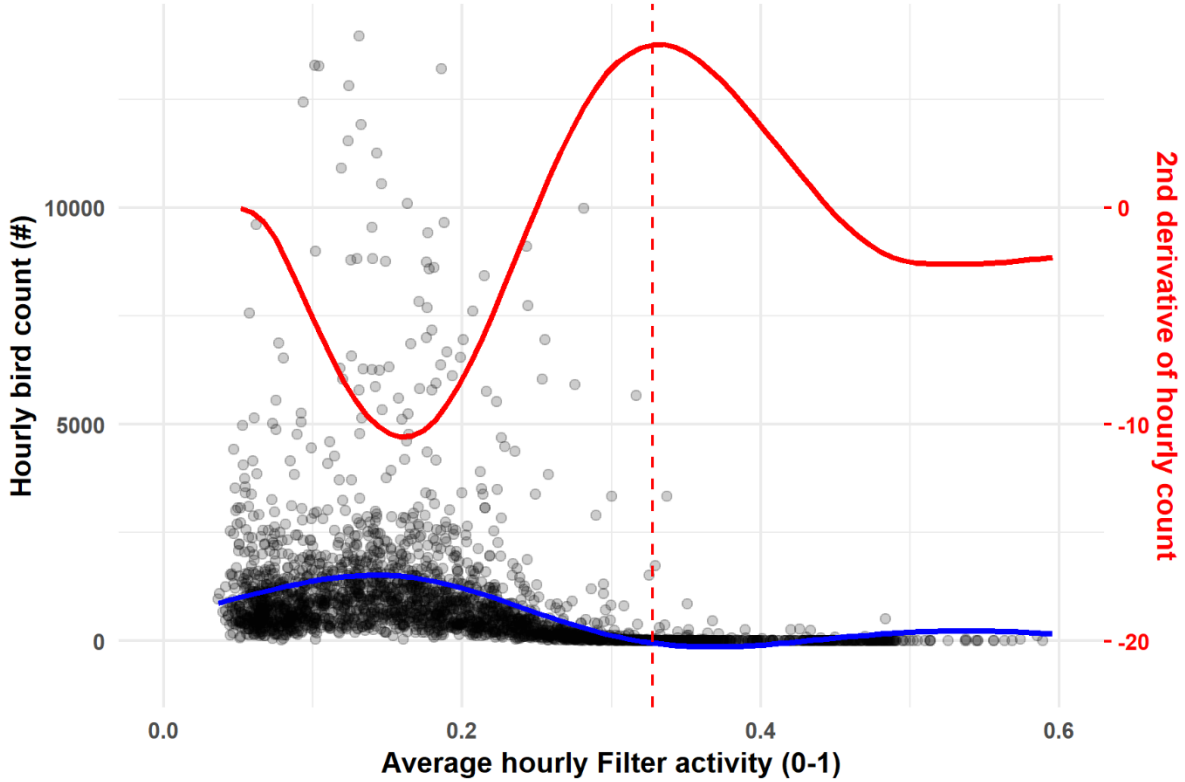

Figure S2 The relation between hourly bird counts and radar filter activity in Luchterduinen radar. Hourly bird counts (left y-axis) at different filter activities (x-axis). Black dots depict all observation hours available. The blue line shows the estimated effect of average hourly filter activity on hourly bird counts (GAM). The red line shows the second derivative of this estimated effect (right y-axis), with the dashed red line depicting the value at which the second derivative was at its maximum, which was used to find the filter activity threshold for data exclusion.

Section S5. Overview of synoptic conditions in North Sea areas surrounding Luchterduinen and Gemini wind farm in support of thermal soaring

Soaring has been observed in both radar and GPS data on some specific days during the summer of 2019 and 2020. In the period 20-07-2020 – 22-07-2020 high a peak in thermal soaring activity occurred in the west and north study areas around the Dutch coast (Figure 3, main text). To explore the synoptic conditions preceding, during and after this event (18-07-2020 – 23-07-2020) we examined synoptic weather charts showing surface pressure and synoptic weather patterns for Europe at 6-hour temporal resolution, downloaded from the KNMI data center (https://www.knmi.nl/nederland-nu/klimatologie/daggegevens/weerkaarten), and the time series of sea surface temperature, air temperature (2 m) and wind speed (10 m) extracted from ERA5 for the two locations. Synoptic weather charts are presented in Figure S3 (taken at 12:00 UTC), and all weather charts for the period are presented in supplementary video S1.
On 18-07-2020 a stationary front is present over the North Sea. By the end of 19-07-2020 a cold front has formed along the Dutch coastline. The cold front leaves behind a trough of low atmospheric pressure at the end of the day and into the following days (solid blue lines), which brings cold maritime wet air from the northwest. The presence of such cold air creates suitable conditions for the development of thermals near the Dutch coast; the air temperature drops and remains below the sea surface temperature for several days (Figure S4.a-b), which drives a flux of sensible heat from the sea to the atmosphere (Markowski & Richardson 2010). Note that during these days the wind speed is not particularly high (Figure S4.c), which provides beneficial conditions for thermal soaring as it reduces the likelihood of thermal disturbance and break up.

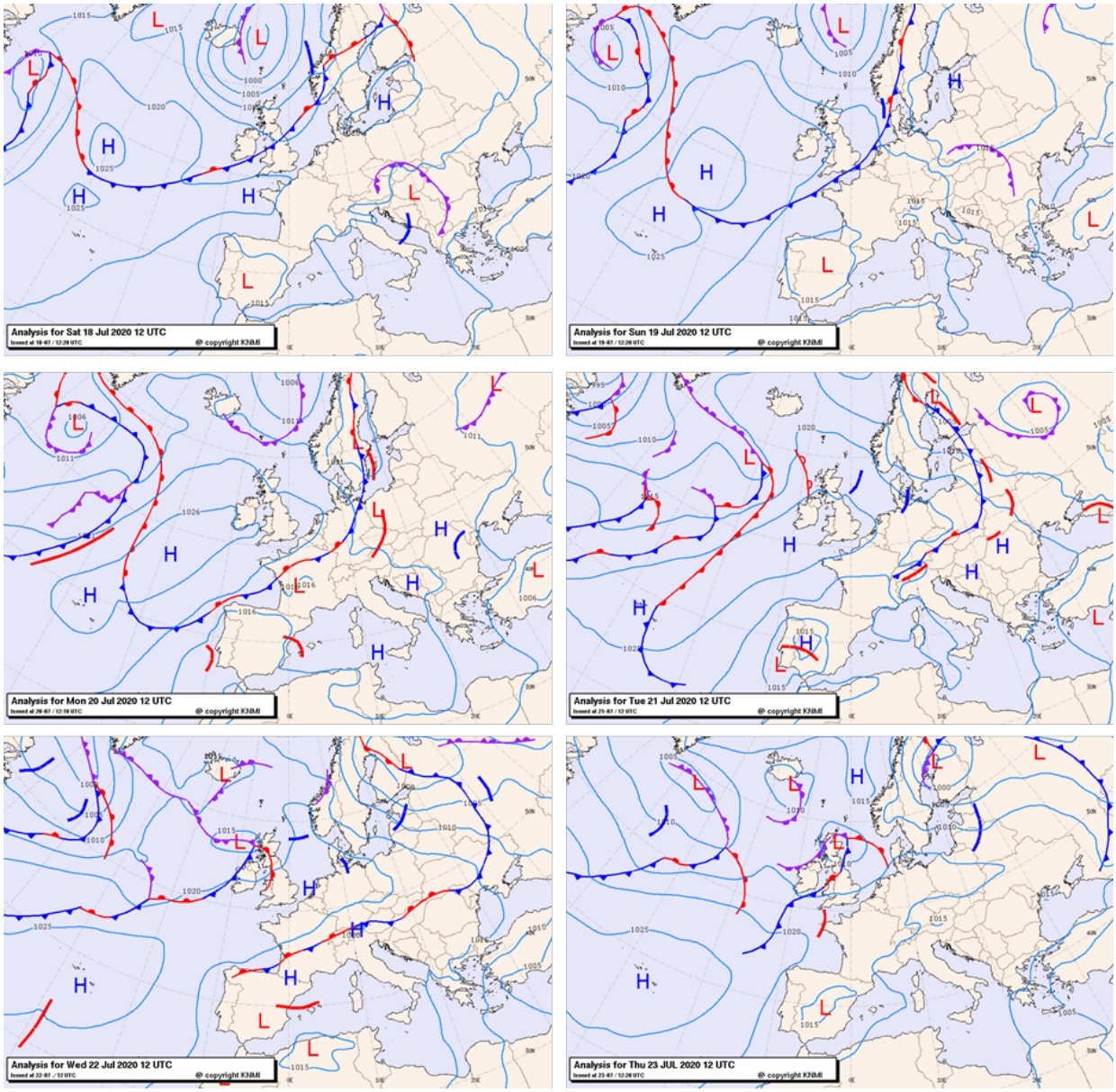

Figure S3. KNMI synoptic weather charts between 18/07/20 and 23/07/20, taken at 12:00 UTC

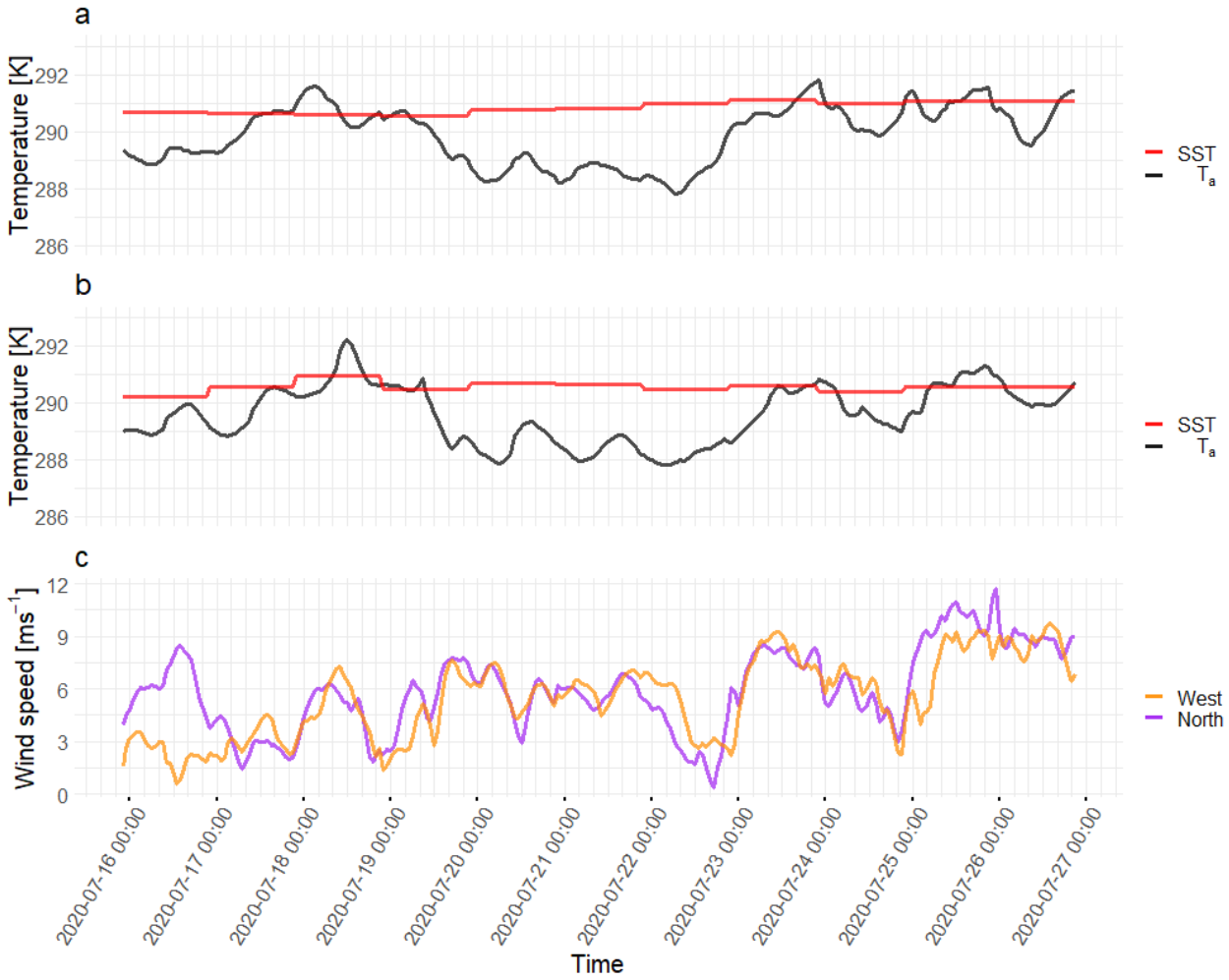

Figure S4. Sea surface temperature (SST) and air temperature at 2 m above surface (T_a) between 16/07/2020 and 27/07/2020 in west study area (a) and north study area (b). Wind speed at 10 m ASL between 16/07/2020 and 27/07/2020 in west and north study areas (c).

Section S6. Remaining temporal autocorrelation in the logistic regression model residuals

Temporal autocorrelation in the model residuals of the proportion of thermal soaring per hour as function of temperature difference, and wind u- and v-components was addressed through a first order autoregressive covariance structure. However, this covariance structure could not completely resolve temporal autocorrelation in the models for the west area radar data. More complex covariance structures (second-/third order autoregressive and moving average autoregressive) did not improve the residuals further. Below is the remaining temporal autocorrelation plot for the west area radar logistic regression models.

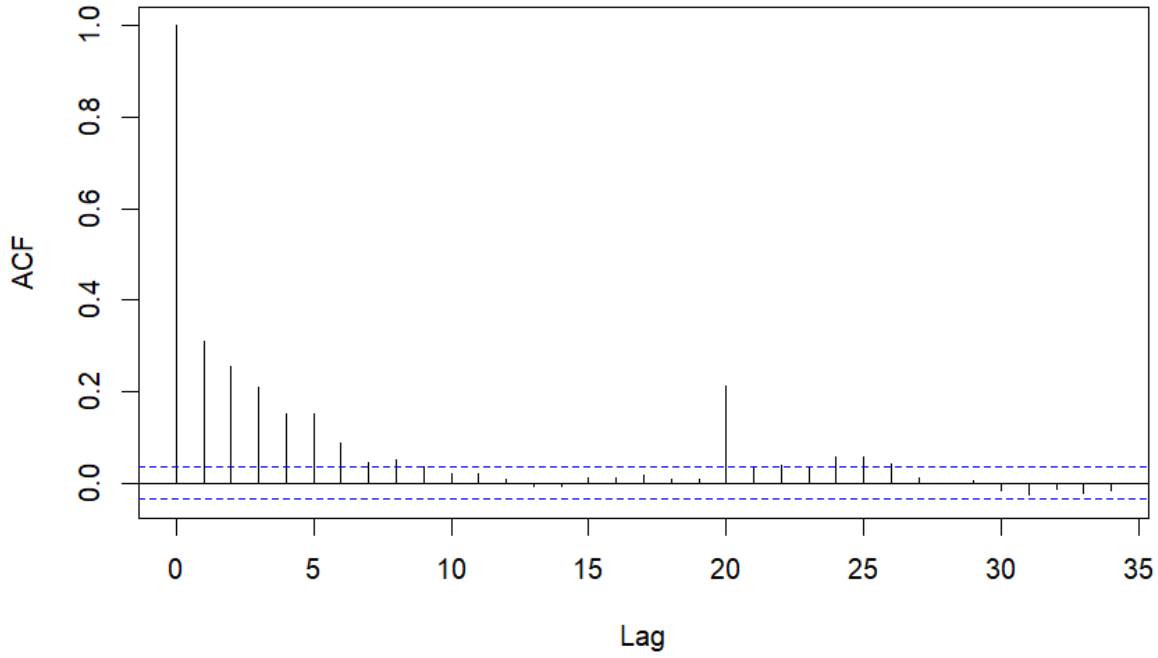

Figure S5 Autocorrelation function for the logistic regression model of proportion of circling tracks as a function of temperature difference between sea surface and air in the west area radar data. The x-axis shows the lag in hours from the observation, the y-axis shows the autocorrelation function. Autocorrelation is present for lag 1-6 and lag 20.

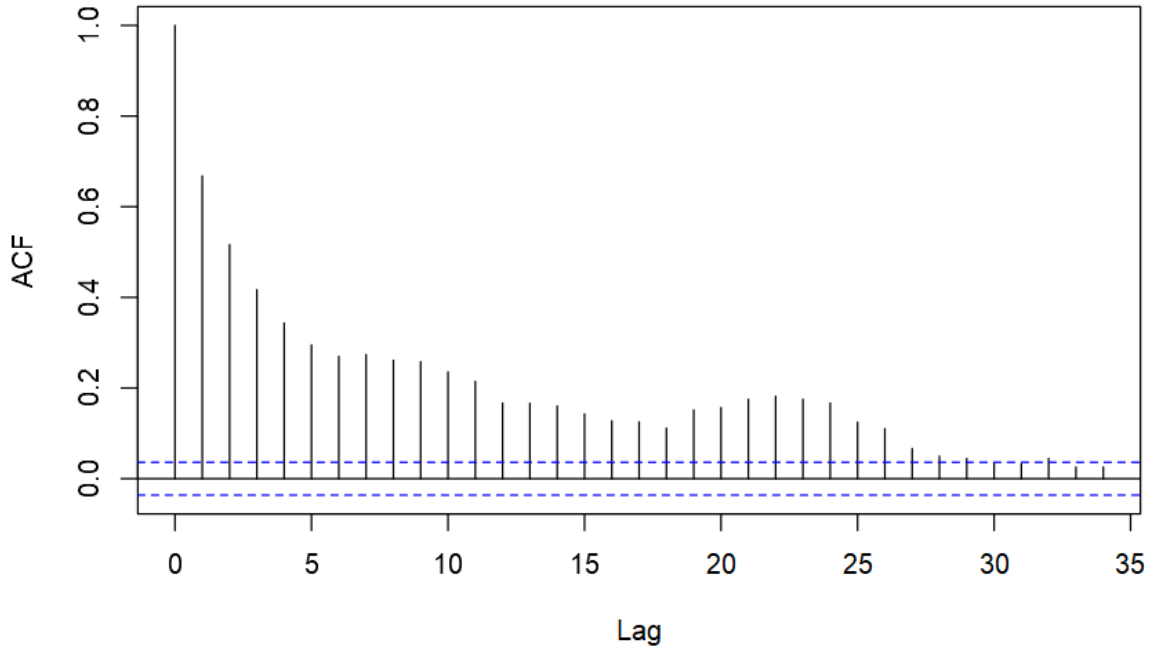

Figure S6 Autocorrelation function for the logistic regression model of proportion of circling tracks as a function of temperature difference between sea surface and air in the west area radar data. The x-axis shows the lag in hours from the observation, the y-axis shows the autocorrelation function. Autocorrelation is present for lag 1-27, with severe auto-correlation for lag 1-9.

LITERATURE CITED

Camphuysen CJ, Fox AD, Leopold MF, Petersen IK (2004) Towards standardised seabirds at sea census techniques in connection with environmental impact assessments for offshore wind farms in the U.K. Report for the COWRIE. Royal Netherlands Institute for Sea Research (NIOZ), Den Burg, Texel. doi:10.13140/RG.2.1.2230.0244

Markowski P, Richardson Y (2010) Mesoscale meteorology in midlatitudes. John Wiley and Sons. doi:10.1002/9780470682104

Reid J, Camphuysen CJ (1998) The European Seabirds at Sea database. In: Spina S, Grattarola A (eds) Proceedings of the 1st meeting of the European Ornithologist's Union. Biol Conserv Fauna 102:291